Impact of Cellulose and Surfactants on Mass Transfer of Bubble Columns

Aida Ahmia, Madjid Idouhar, Kritchart Wongwailikit, Nicolas Dietrich, Gilles Hébrard

Impact of surfactants and cellulose on the hydrodynamic behavior and liquid-side mass transfer coefficient of a bubble column

A.C.Ahmia[1,2,4], M.Idouhar[1], K.Wongwailikit[3,4], N.Dietrich[4], G.Hébrard[4]

[1] Laboratory of Applied Organic Chemistry, Faculty of Chemistry, USTHB, 16111 Algiers, Algeria
[2] Centre de Développement des Energies Renouvelables, CDER, 16340 Algiers, Algeria
[3] Department of Environmental Engineering, Faculty of Engineering, Chulalongkorn University, 10330 Bangkok, Thailand
[4] INSA, UPS, INPT; LISBP, Université de Toulouse, Toulouse, France

E-mail :hebrard@insa-toulouse.fr

ABSTRACT

The aim of this paper is to present and understand the effect of surfactants, cellulose and their combination on the hydrodynamic behavior and the liquid side mass transfer coefficient of a bubble column. For that purpose, the effect of liquid properties on the interfacial area and the liquid-side mass transfer coefficient was investigated. Bubbles were generated in a small-scale bubble column having an elastic membrane with a single orifice as the gas sparger. Different aqueous solutions containing surfactants (SDS) and cellulose (MCC) were investigated and characterized concerning their surface tension and viscosity. The interfacial areas (a) were calculated from the bubble diameters (D_B), the bubble frequencies (f_B) and the terminal bubble rising velocities (U_B). The liquid-side mass transfer coefficients (k_L) were calculated from the volumetric mass transfer coefficients (k_La) measured by the dynamic method. In the range of concentration under test, the experimental results showed that the addition of MCC to the studied liquid phases did not affect the mass transfer coefficient. However, the addition of SDS to water and to MCC in water system decreases the mass transfer coefficient.

Keywords: Surfactant; Microcrystalline cellulose; Bubble generation; Interfacial area; Volumetric mass transfer coefficient; Liquid-side mass transfer coefficient; Superficial gas velocity.

1. INTRODUCTION

Bubble Columns are usually encountered in chemical, pharmaceutical, petrochemical and metallurgical industries as multiphase reactors due to their simple construction, low cost and ease of operation [1]. In the majority of wastewater treatment plants (WWTPs), the activated sludge (biological treatment in the aerated tank) is employed for the degradation of organic pollutants present in wastewaters. A source of dissolved oxygen by injecting air bubbles is then required to ensure the metabolism of the microorganisms which use the organic matter as a source of nutrition, and then degrade it [2]. In the gas–liquid reactors, mass transfer must be maximum for a given power consumption [3]. In conventional wastewater treatment plants, air supply used in activated sludge treatment can represent up to 70% in terms of energy expenditure [4][5]. Therefore, accurate determination of mass transfer parameters is of prime interest to avoid over- or under-estimating of the required oxygen supply to the process [4]. The process optimization involves a good understanding of how the different operational parameters influence the aeration efficiency of the system [5].

Most part of investigations in bubble columns have been performed for aqueous systems. Based on a large number of studies on oxygen transfer in clean water, the American Society of Civil Engineers (ASCE) standard was established to measure the oxygenation capacity of aeration devices in clean water [6]. The impacts of physical variables such as temperature, reactor geometry, pressure, surface tension, mixing and viscosity on oxygen transfer in clean water are well documented and understood. However, the presence of real contaminants into raw wastewater is not yet well evaluated thereby it strongly impacts the efficiency of the process. To improve the productivity of the reactors, it is required to well study and understand the relationship between the mass transfer rate and the liquid phase contents.

The most commonly occurring contaminants accumulating at the environmental gas/liquid interfaces are surfactant compounds. Because of their wetting, dispersing, solubilizing and foaming properties, they enter in the formulation of pharmaceuticals, cosmetics, pesticides, and household products [2][7]. Surfactant world production was 1.7 million tons in 1984. It increased from 9.3 million tons in 1995 to over 13 million tons in 2008. Their compound annual growth rate (CAGR) is increasing until now [2]. Thus, their presence in the aeration tank of WWTPs must be absolutely considered. Surfactants are amphiphilic compounds having both hydrophilic and hydrophobic groups [2]. Due to their nature, surfactants accumulate at the interface of liquid-gas systems and lower the interfacial tension. This last decreases with increasing the surfactant concentration until the critical

micelle concentration (CMC). The ability of surfactant to alter oxygen mass transfer has been vastly considered in literature.

Loubière and Hébrard (2004) explored the effect of liquid surface tension on the bubble formation from both rigid and flexible orifice. Results indicated that the effect of surface tension on the generated bubbles depends on whether the bubbles are produced from a rigid or a flexible orifice [8]. Alves et al. (2004) investigated the effect of Polyethylene glycol surfactant on the average mass transfer coefficient in an aerated stirred tank. Results indicated that bubbles in surfactant solution behave as rigid bubbles, while bubbles in tap water behave closer to having a mobile interface [9]. Painmanakul et al. (2005) studied the effect of surfactants on the mass transfer parameters in aqueous solutions with Sodium dodecyl sulfate anionic surfactant and Lauryl dimethyl benzyl ammonium bromine cationic surfactants in a small scale bubble column. Results showed that the presence of surfactants affects the bubble generation phenomenon [10]. Rosso et al. (2006) studied the effects of interfacial surfactant contamination on bubble gas transfer. A gas transfer reduction of 30–70% of pure water values in surfactant solutions was shown [11]. Sardeing et al. (2006) examined the effect of anionic, cationic and non-ionic surfactants on the mass transfer rate of bubbles in a small-scale bubble column. Results revealed that whatever the liquid phase, three zones are found on the liquid-side mass transfer coefficient variation with the bubble diameter [12]. Hébrard et al. (2009) studied the effect of high concentration of surfactants on liquid side mass transfer coefficient in free gas–liquid interface. A reduction in the mass transfer coefficient with an increase of surfactant concentrations was detected as well as a plateau when the concentration reaches critical micelle concentration [13]. Jamnongwong et al. (2010) inspected the effect of presence of various substances commonly encountered in biological media. Results showed that in presence of surfactants, for all liquid phases under test, oxygen diffusion coefficients decreased when compared to clean water [14]. Takagi and Matsumoto (2011) reviewed the recent investigations associated with subsequent variation of bubble behavior due to the surfactant adsorption/desorption on the bubble surface. They concluded that the presence of surfactants influences the small-scale behavior of each bubble [15]. Kotti et al. (2013) considered the effects of the presence of anionic and cationic surfactants in the liquid phase and the hydrodynamic regime of the bubble flow on the oxygen transfer rate in an electroflotation process. They revealed that the specific interfacial area tends to increase by the addition of cationic surfactant and decreases with the anionic surfactant [16]. Jimenez et al. (2014) used a powerful technique, based on the Planar Laser Induced Fluorescence (PLIF)

technique to locally visualize and quantify the impact of surfactants in wastewaters on hydrodynamics and oxygen mass transfer. Bubbles have been found to be more spherical with a reduced rise velocity in the presence of surfactants up to the CMC. Hydrodynamic characteristics were found to be practically constant above the CMC, even if the oxygen mass transfer decreased [4]. McClure et al. (2015) compared the influence of surfactant addition and sparger design on the mass transfer, the gas holdup and bubble size distribution in a bubble column. Results showed that addition of surfactants cause an approximately threefold decrease in mass transfer coefficient [17]. Aoki et al. (2015) investigated the effect of concentration of surfactant on the rate of mass transfer for single rising bubbles. They used Triton X-100 as surfactant and showed that for small bubbles the mass transfer rate decreases with increase of surfactant concentration. Furthermore, they proved that the surfactant adsorbs only in the bubble tail region [18]. Haghnegahdar et al. (2016) investigated the effect of surfactant on the bubble shape and mass transfer in a milli-channel using high-resolution microfocus X-ray imaging. Results showed that the presence of surfactants causes a change of the bubble shape and leads to a slight increase of the liquid film thickness around the bubble. They also concluded that the presence of surfactant has a more significant impact on the dissolution rate of small bubbles [19].

Hydrodynamic behavior and mass transfer parameters of other types of medium such as non-Newtonian media have been widely investigated. The microcrystalline cellulose is a significant fraction of the solid organic matters [20]. Its presence as a non-Newtonian fluid in WWTPs is believed to be mainly from toilet paper. This last is one of the mostly used ubiquitous personal hygiene products, particularly in Northern Americas and European countries. The first packaged toilet paper was commercialized in New-Jersey by Joseph Gayetty in 1857. Paper wastes are mostly originated from wood pulp or cotton which consists of 90–99% cellulose fibers [21]. A part of paper wastes is precipitated in the primary clarification tank implanted to separate suspended solids from sewage. Then, cellulose could be a potential resource removed easily from wastewater by for instance sieving [20]. It can be used as a renewable and biodegradable resource for the production of biofuels and others functional chemicals such as cellulose acetate and cellulose ether [21]. The second part of paper wastes is transported to the aerated tank where it is hardly degraded because it needs first to be hydrolysed before it can be metabolized. The biological hydrolysis of cellulose may take much more time than the usual hydraulic retention time (HRT < 12 h) for conventional biological treatment process and it strongly depends on temperature [20]. The ability of

cellulose present in the aerated tank to alter oxygen mass transfer has not been much considered in literature compared to surfactant.

Popovic and Robinson (1987) studied the specific interfacial area in an external circulation-loop airlifts and a bubble column using a carboxymethyl cellulose/sulphite solution. Results showed that the specific interfacial areas for the studied systems was found to be two- to three fold smaller than in the non-viscous Newtonian systems previously investigated by the authors [22]. Guo-Qing et al. (1995) [23] and Vasconcelos et al. (2003) [24] showed that systems with higher viscosity such as carboxymethyl cellulose exhibited a lower k_La than those running with lower viscosity mediums. Roberts et al. (2011) investigated the effects of water interactions in cellulose suspensions on mass transfer and saccharification efficiency at high solids loadings. Results showed that increasing water constraint is related to the increased viscosity of the fluid in the suspensions [25].

Given that the presence of surfactant compounds and MCC is simultaneously unavoidable in the aerated tanks of WWTPs, the study of their combination on the hydrodynamic behavior and liquid-side mass transfer coefficient in a bubble column should be important to well estimate the required oxygen supply to the aeration process. In keeping with this context, and for the first time, this paper study the effect of surfactants and MCC combination on the hydrodynamic behavior and the mass transfer parameters. The investigation is based on the determination of the effect of liquid properties on bubble generation phenomenon, interfacial area and liquid-side mass transfer coefficient. Bubble column having an elastic membrane with a single orifice as gas sparger was used in this work. It offers the possibility to well master the interfacial area provided by the bubble train allowing an accurate estimation of the liquid side mass transfer coefficient.

2. MATERIAL AND METHODS

A schematic overview of the experimental device is represented in Figure 1. The experiments are carried out in a glass bubble column (1) of 0.05 m in diameter and with a liquid height (H_L) of 0.20 m. The column is immovable into a doublewall glass vessel (2) of 0.40 m in width, 0.40 m in length and 0.30 m in height. The bubble diameters and their terminal rising velocities used to calculate the specific interfacial area have been determined thanks to image analysis and high speed camera (3). The temperature in the bubble column is

measured by means of a thermometer (4). Nitrogen (5) is employed for oxygen elimination in the liquid phase. Piece of 0.60 m diameter of an industrial rubber membrane sparger (6) is used as gas sparger. Bubbles are generated by a single puncture located at the membrane center. The membrane is assembled on a circular clamping ring (7) composed of two jaws; this fixing system coupled with the use of a dynamometric spanner enables the same initial tension to be applied, thus giving reproducible results [10]. The gas flow is monitored by a pressure gauge (8) and regulated by a gas flow meter (9). A three-way valve is used to inject either air or nitrogen (10). An oxygen microsensor (11) is used to measure the change in dissolved oxygen concentration. The double wall vessel is filled with water and a white plywood plate (13) is introduced to improve the image acquisition quality. Acquisition computer is connected to visualize and treat the results (14). SDS, MCC and SDS/MCC solutions are introduced at the top of the bubble column.

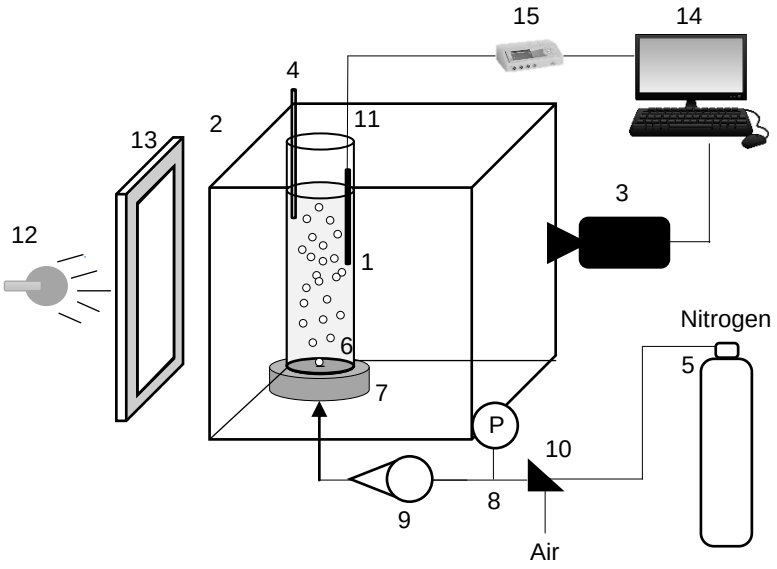

Figure 1. Schematic overview of the experimental device

To understand the effect of cellulose, surfactants and their combination on the liquid-side mass transfer coefficient, several liquid phases have been prepared and characterized. Compressed air and nitrogen from laboratory lines were the gas phases used in our work. Note that, a great care was taken for the cleaning and rinsing procedure of vessels to avoid contamination of surfactant. To prepare synthetic liquid phases, distilled water was combined with two types of compounds: (i) a microcrystalline cellulose (MCC); (ii) an anionic surfactant named sodium dodecyl sulfate (SDS), synonymously sodium lauryl sulfate (SLS). They were selected as commonly found in the biological tanks of WWTPs. The SDS used

(CAS Number 151-21-3) and the MCC (CAS Number: 9004-34-6) were purchased from Sigma Aldrich. Three solutions of SDS, four solutions of MCC and four solutions of SDS/MCC combination were tested. SDS1, SDS2 and SDS3 represent the solutions containing 1 g/L, 2 g/L and 2.59 g/L of SDS respectively. MCC0.5, MCC1, MCC2 and MCC5 represent the solutions containing 0.5 g/L, 1 g/L, 2 g/L and 5 g/L of MCC respectively. SDS/MCC 0.5, SDS/MCC1, SDS/MCC2 and SDS/MCC5 represent the solutions containing 1 g/L of SDS and 0.5 g/L, 1 g/L, 2 g/L and 5 g/L of MCC respectively. Given that the liquid phases under study are dilute aqueous solutions, their density can be assumed to be equal to that of tap water (997 kg/m^3). The viscosity of SDS solutions also can be assumed to be equal to that of tap water (10^{-5} Pas) [14]. Therefore, the liquid-phases characterization will consist on the determination of the static surface tensions, the critical micelle concentration (CMC) and the adsorption parameters for SDS solutions; the rheology for MCC solutions; and the dissolved oxygen concentration at saturation (C^*) which depends on the temperature for both SDS and MCC solutions.

At the contrary of the dynamic surface tension measurement, the surface age is not taken into account in the static surface tension measurement. This last can be accomplished by two methods: (i) the static method of Du Noüy, using a KRÜSS K6 Force Tensiometer. This method is based on slowly lifting a ring, often made of platinum, from the surface of a liquid; (ii) the static method based on the pendant drop using KRÜSS DSA25 Drop Shape Analyzer. Both methods gave the same results.

To calculate the critical micelle concentration (CMC) for surfactant aqueous solutions, static surface tension has to be determined for a number of different concentrations. When the surfactant concentration increases, the surface tension tends to decrease until levelling off. Here, the solution is saturated in surfactants compounds and there is micelles formation. The CMC is then reached. Deduced from the curve linked the surfactant concentrations and the surface tensions, the CMC is reported.

To characterize the adsorption parameters at a gas–liquid interface, the Langmuir theory is used [12][8]. The kinetics of adsorption and diffusion of the surfactant molecules towards the bubble interface can be defined by using the equations (1) and (2):

$$S_e = \frac{\Gamma_e}{\Gamma_\infty} = K\frac{C}{1+KC} \quad (1)$$

$$\sigma_{L,O} - \sigma_L \approx RT_a\Gamma_\infty Log(K) + RT_a\Gamma_\infty Log(C) \quad (2)$$

Where *Se* is the surface coverage ratio at equilibrium, *C* is the solute concentration in the liquid phase, *K* is the adsorption constant at equilibrium, Γ_∞ is the surface concentration at saturation, $\sigma_{L,0}$ is the surface tension when the solvent is pure and *Ta* the adsorption temperature. The surface concentration at saturation Γ_∞ is determined using the slope of the curve linked the surface tension and Log(C) described in Figure 2. From the values of C, K and Γ_∞, the surface coverage ratio *Se* is deduced. Given its importance, *Se* is a parameter which can be chosen to classify the bubbles according to their interface nature [12]:

· Se =0 corresponds to an interface free of surfactants,

· Se=1 corresponds to an interface saturated with surfactants,

· 0<Se<1 corresponds to a non-saturated interface.

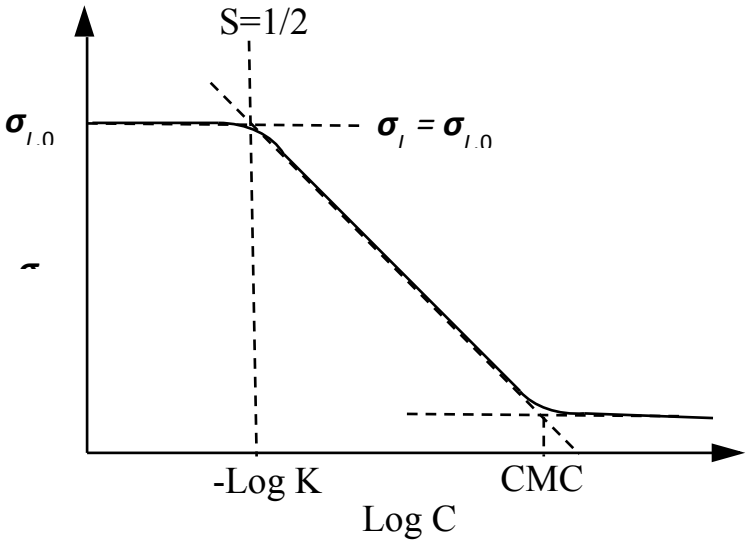

Figure 2. Diagram for determining the characteristic adsorption parameters

Because of the Newtonian behavior of surfactant solutions, the viscosity of their liquid phases is not modified. However, the microcrystalline cellulose solutions have a non-Newtonian fluid behavior, the viscosity of the liquid-phases changes with concentration changes. That brings us to study the rheology of MCC solutions. A rheological measurement consists on determining the longitudinal pressure loss associated to the liquid flow rate through a capillary tube of known geometry [5]. To determine the rheological behavior of MCC solutions under study, a Thermo Fisher Scientific HAAKE MARS rheometer-system equipped with a plate-plate geometry was used. The Ostwald-de Waele rheological parameters were determined using (3), where K represents the flow consistency index and n the flow behavior index.

$$\eta = K\gamma^{n-1} \quad (3)$$

As shown in Figure 1, bubbles are photographed with a 64-bit Pylon Viewer fast camera [acA1920-155um] that can shoot up to 390 frames per second. The lighting is accomplished by a LED lamp. The introduction of a white plywood plate into the reactor increases the contrast of the images. Images are visualized on the acquisition computer and are treated with the ImageJ software. Figure 3 presents a typical sequence of image treatment which is based on a transformation of the acquired image into a binary image. Different arithmetical and geometrical operations as filling the holes followed the binarization to give a uniform surface treatment and to remove superfluous images.

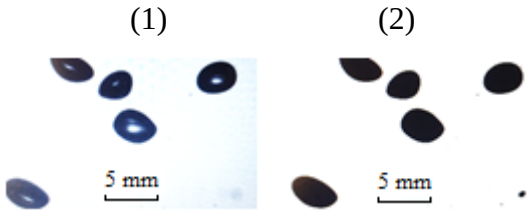

Figure 3. Typical sequence of image treatment: (1) image acquisition; (2) image binarization

Afterward the images acquisition and treatment, the effect of liquid phase concentrations on hydrodynamic and mass transfer parameters can be determined.

At low gas flow rates, bubbles are spherical and Eq. (4) is considered to calculate the diameter. At high gas flow rates, bubbles become ellipsoidal and Eq. (5) is considered to calculate the diameter after the measurement of the geometrical characteristics [10]. An average bubble diameter is deduced from the measurement of 70 to 100 bubbles diameter.

$$D_B = \sqrt{\frac{4 \times A_B}{\pi}} \quad (4)$$

$$D_B = \sqrt[3]{(l^2 \times h)} \quad (5)$$

The bubble frequency (f_B) can be calculated using two methods: (i) the ratio of air flow rate to bubble volume; (ii) the direct counting of bubbles on the image sequence. Jamnongwong et al. [3] found a good agreement between both methods. The first method was used in this work. The bubble formation frequency is determined as (6):

$$f_B = \frac{q}{V_B} \quad (6)$$

Where V_B is the average detached bubble volume and q is the gas flow rate. Note that a gas flow rate of 1.16 ml/s is fixed whatever the experiments. This low value hinders any surface deformation.

The terminal rising bubble velocity (U_B) can be estimated via two methods: (i) by measuring the distance between two frames; (ii) by following the variation in the bubble extremity coordinates with time. In this work, the first method was used. The terminal rising bubble velocity is determined as (7), where ΔD is the bubble spatial displacement between t = 0 and t = T_{frames} = 1/100 s.

$$U_B = \frac{\Delta D}{T_{frames}} \tag{7}$$

The specific interfacial area (a) is defined as the ratio between the bubble surfaces (S_B) and the total volume in the reactor (V_{Total}) [10] [12] as in (8), where H_L and A are respectively the liquid height (H_L = 0.20 m) and the cross-sectional area (A = 1.5 10^{-3} m^2). The number of bubbles (N_B) is deduced from the terminal rising bubble velocities (U_B) and the bubble formation frequency (f_B) previously determined.

$$a = N_B \frac{S_B}{V_{Total}} = f_B \frac{H_L}{U_B} \frac{S_B}{AH_L + N_B V_B} \tag{8}$$

Depending on the bubble shape, the bubble surfaces are calculated:

- For spherical bubble (9):

$$S_B = \pi . d_B^2 \tag{9}$$

- For ellipsoidal bubble (10), where e is the ratio between h and l.

$$S_B = 2\pi\left[\frac{l^2}{4} + \left(\frac{l^2}{4} \times \frac{l}{2e} ln \frac{(1+e)}{(1-e)}\right)\right] \tag{10}$$

The superficial gas velocity (Ug) is defined as the average velocity of the gas that is sparged into the column. In calculations, superficial gas velocity is simply expressed as the volumetric flow rate (q) divided by the cross-sectional area of the column (A). Flow rates of 0.55 ml/s, 1.16 ml/s, 2 ml/s and 2.5 ml/s were chosen to study the influence of superficial gas velocity on mass transfer parameters.

The volumetric mass transfer coefficient (K_{La}) can be appreciated through two methods: (i) the sulfite static method based on a mass balance on sulfite sodium (Na_2SO_3) concentration

during aeration time [10][3][12]; (ii) the classical method named the non-stationary or the dynamic method [10][14][13]. In this work, the classical method was used. It consists in passing nitrogen through the liquid phase in order to remove the oxygen content and to substitute it with air at the beginning of the experiment. The oxygen concentration in the liquid phase is measured with an oxygen microsensor. In our experiments, UNISENSE microsensor which is a miniaturized Clark-type oxygen sensor was used. The sensor is related to a high-sensitivity picoammeter, allowing the resulting reduction current from the oxygen penetration to be converted into a signal. The conversion of this signal into an equivalent concentration of oxygen *(C_L)* is assured by considering a linear conversion and by multiplying with the atmospheric level solubility. During the experimental route, sufficient time is available to reach the oxygen saturation *(C^*_L)* in the liquid. The response time of the used probe is fixed to be as low as 50 ms, which corresponds to the experimental error estimated to $\pm 2\%$ for the volumetric mass transfer coefficient determination. To apply this method, several assumptions are made: the liquid phase is perfectly mixed, the response time of the probe is negligible and the oxygen depletion from gas bubbles is negligible. As the oxygen concentration increases, the mass transfer rate is given by the equation (11):

$$\ln(C_L^* - C_L) = \ln(C_L^*) - k_{Lat} \quad (11)$$

The volumetric mass transfer coefficient is then deduced from the slope of the curve linking the variation of ln ($C_L{}^* - C_L$) with time (*t*).

However, the signal (S) of the polarographic probe can be directly used for calculating the volumetric mass transfer coefficient [14]. Indeed, the volumetric mass transfer coefficient in the liquid phase is deduced from the slope of the curve described by (12):

$$Ln\frac{S^*-S}{S^*-S_0} = -k_{Lat} \quad (12)$$

The volumetric mass transfer coefficient is the product of the liquid-side mass transfer coefficient (K_L) and the specific interfacial area. The most commonly method used to estimate the liquid-side mass transfer coefficient [10][14][12][13] is by using the equation (13):

$$k_L = \frac{k_{La}}{a} \quad (13)$$

3. RESULTS AND DISCUSSION

Concentrations of the liquid phases and their characterization are reported in Table 1. According to the experimental values of surface tension and taking account for experimental uncertainties, the surface tensions of MCC solutions do not vary from the one of tap water (σ_L = 72.2 mNm^{-1}). On the contrary of inorganic substances addition [14][8], adding surfactants to tap water strongly lowers the surface tensions (σ_L = 39.0–43.5 mNm−1). When the surfactant concentration increases, the surface tension tends to decrease until saturation of the solution with surfactants compounds. Here, the CMC is reached and the surface tension remains constant above this concentration. Change in surface tension of SDS and SDS/MCC solutions is believed to affect hydrodynamics and oxygen mass transfer. The critical micelle concentration of SDS found (2.01 g/L) is slightly higher to these found in literature (1.9 g/L) [10][14][12]. The value of the surface coverage ratio *se* is assumed to be equal to 0 in the case of water. However, *se* increases with the surfactant concentration in the liquid phase. Furthermore, the surface coverage ratio se is equal to 1 when the concentration is equal or higher than the critical micelle concentration. Here, the interface is saturated.

Table 1. Properties of liquid phases under test

Liquid phase	*C* (mol/L)		*C* (g/L)		*M* (g/mol)	σ_L (mN/m)	*CMC* (gl/L)	*C** (mg/L)	*K* (m^3/mol)	Γ_∞ (mol/m^2)	Se
	SDS	MCC	SDS	MCC							
Tap water	0	0	0	0	18	72.2	-	8.81	-	-	0
SDS1	3.5×10^{-3}		1.00			43.5		9.18			0.9
SDS2	7×10^{-3}	0	2.01	0	288.37	39	2.01	9.13	6.25	3.50×10^{-6}	1
SDS2.59	9×10^{-3}		2.59			39		9.12			1
MCC0.5		$3\ 10^{-3}$		0.50		72		8.98			
MCC1	0	$6\ 10^{-3}$	0	1.00	162.14	72.2	-	9.01			
MCC2		$1.2\ 10^{-2}$		2.00		72		8.89	-	-	-
MCC5		$3\ 10^{-2}$		5.00		72.1		8.86			
SDS/MCC0.5		3 10-3		0.5		43.7		9.06			
SDS/MCC1	$3.5\ 10^{-3}$	6 10-3	1	1	-	43.8	-	9.15	-	-	-
SDS/MCC2		1.2 10-2		2		43.6		9.18			
SDS/MCC5		3 10-2		5		43.7		9.20			

To more understand the microcrystalline cellulose rheology, concentrations ranging from 0.5 to 5 g/L of MCC solutions are studied. Variation of the apparent liquid viscosity as a function of the applied shear rate is shown in Figure 4. The obtained Ostwald-de Waele rheological parameters are presented in Table 2. Results show that the liquid apparent viscosity decreases as the applied shear stress increases. It can also be shown that the

362 microcrystalline cellulose liquid apparent viscosity and the consistency index *(K)* increase
363 simultaneously with the MCC concentration. This result can be explained by a higher number
364 of interactions between cellulose particles that consequently move less freely and exert more
365 resistance to flow. On the opposing, it is observed that the flux index *(n)* decreases when the
366 MCC concentration increases, thereby highlighting the shear-thinning character of the MCC
367 liquid (decrease in viscosity with an increase in shear rate). From the values of *n* obtained for
368 all concentrations ($0<n<1$), it can be concluded that the MCC liquid phases are a highly
369 viscous pseudo-plastic solutions.

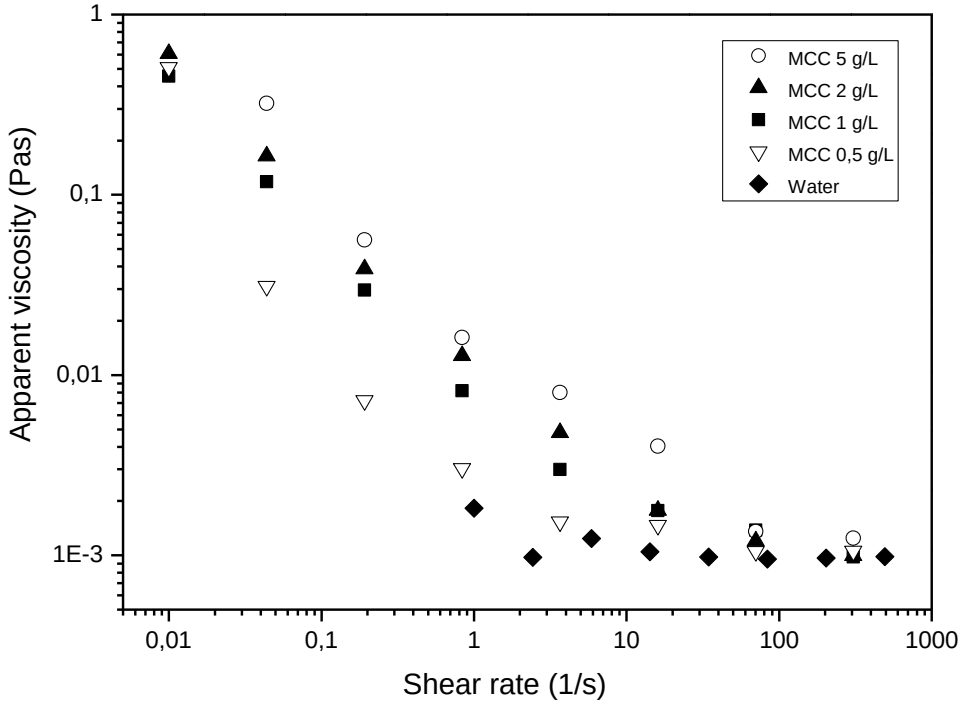

370

371 Figure 4. Rheology of microcrystalline cellulose liquids

372 Table 2. Results of the multiple regression analysis on the rheology experimental data

Parameter	Liquid phase			
	MCC0.5	MCC1	MCC2	MCC5
K (Pa s)	0.013	0.018	0.024	0.029
n	0.451	0.405	0.381	0.171

373

374 In the part below, the effect of liquid phase concentrations on hydrodynamic and mass
375 transfer parameters is considered. All the data reported and commented have been obtained
376 for a constant superficial gas velocity of 7.73×10^{-4} m s^{-1}.

The relation between the detached average bubble diameters and the liquid phase concentrations for each solution are shown in Figure 5. The result shows that the average bubble diameters obtained with SDS, MCC and SDS/MCC solutions were lower than that obtained with the tap water, except for SDS/MCC at 2 and 5 g/L where the average diameter was greater than that of water. This result can be explained by the coalescence between bubbles due to the high viscosity of the solutions. For SDS solutions, it was observed that the average bubble diameter decreased as the concentration increased due to the differences in term of dynamic surface tensions. The effect was also observed by Loubière and Hébrard [8] and Painmanakul et *al* [10] reporting that the bubble diameter of SDS solution with the surface coverage ratio (*Se*) equal to 1 was smaller than those with low *Se*, which clearly demonstrates the modification of the bubble diameters due to the surfactant concentration. For SDS concentrations above the CMC (SDS2.59), the bubble diameter remained practically constant. For MCC solutions, firstly the average diameter initially decreased but then increase with the concentration remained constant after the concentration was above 2 g/L. For SDS/MCC solutions, the bubbles diameter seems to be independent of the concentration of MCC as the MCC presenting in the liquid phase could adsorbed a certain amount of SDS leading to a limitation of surfactants effect on the bubble sizes. Whatever the solutions under test, the change of bubbles diameter compared with that of water is certainly due to the change in surface tension for SDS solutions, change in viscosity for MCC solutions, and both surface tension and viscosity for SDS/MCC solutions.

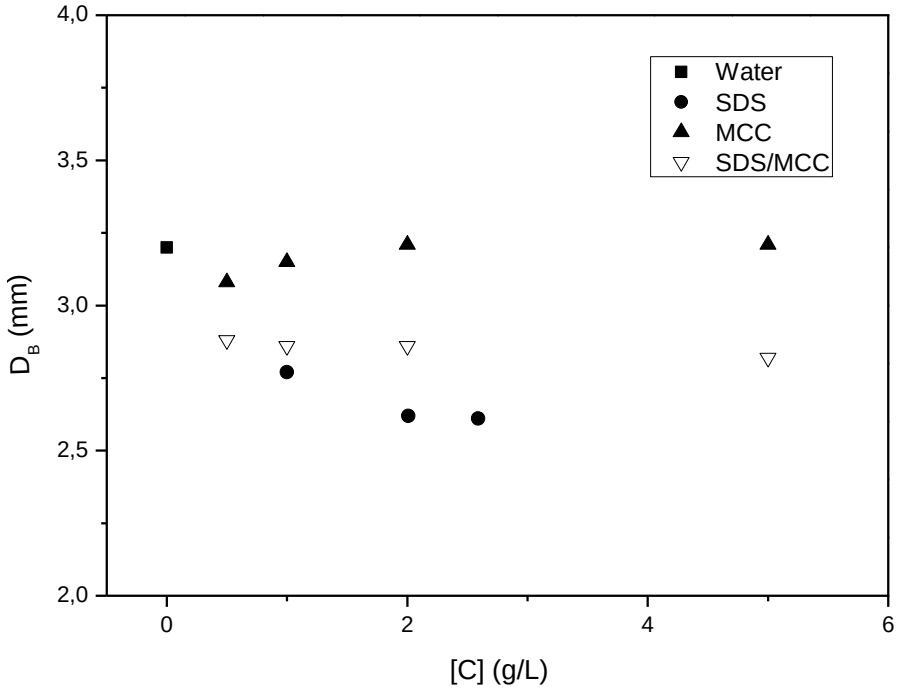

Figure 5. Bubble diameter versus liquid phase concentration

Variations of the rising bubble velocity with the bubble diameter generated for each SDS, MCC and SDS/MCC solutions are plotted in Figure 6. Over the whole bubble diameter range (2.62 – 3.2 mm), the terminal rising bubble velocities obtained varies between 0.21 and 0.28 $m.s^{-1}$ and are included to those given by Grace and Wairegi [26]. These results show that the terminal rising bubble velocity can be affected by the presence of SDS, MCC and their combination; For SDS and SDS/MCC solutions, the terminal rising bubble velocities are respectively reduced from 0.28 to 0.25 $m.s^{-1}$ and from 0.28 to 0.21 $m.s^{-1}$ compared to those of tap water. This diminution is certainly due to the liquid film generated by surfactants compounds around the bubbles which prevents bubbles from moving faster.

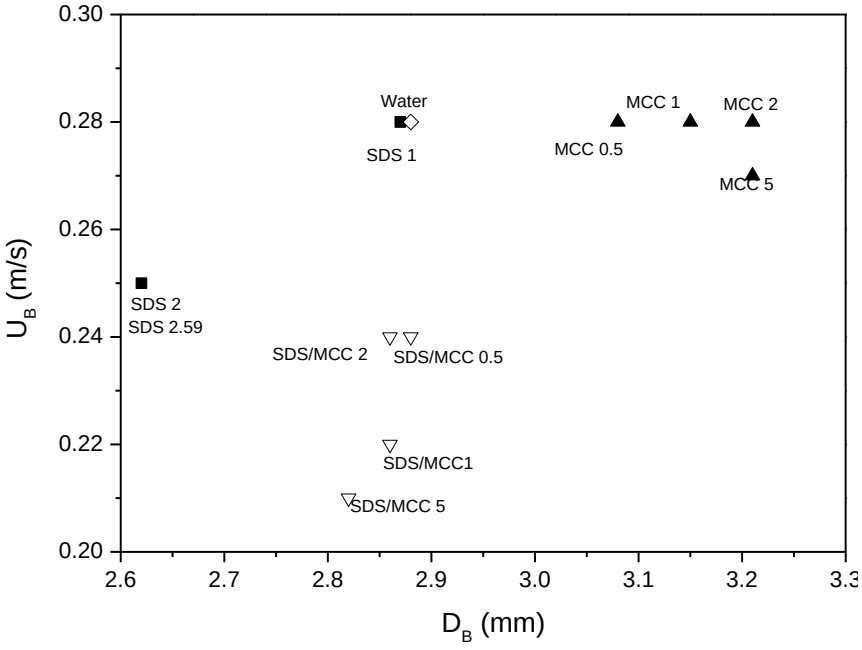

Figure 6. Terminal rising bubble velocity versus bubble diameter

The relation between the interfacial area and the concentration for each SDS, MCC and SDS/MCC solutions is shown in Figure 7. Results show that the values of the interfacial area vary between 4.97 and 7.97 m^{-1} for the concentration varying between 0.5 and 5 g/L. Except the MCC liquids, whatever the SDS and SDS/MCC concentration in the liquid phase, the value of interfacial areas were higher than that of water. For MCC liquid phases, the interfacial area decreases when the MCC concentration increase. This result is undoubtedly due to the increase in the viscosity of the solution as reported in Figure 5 correlating to an

increase in bubble sizes as reported on Figure 6. The interfacial areas related to surfactant solutions are significantly higher than that found for tap water. This great influence on the interfacial area can be explained by the bubble size decrease in presence of surfactant compounds. The result consistent with that obtained by Painmanakul et al [10]. For the SDS and SDS/MCC solutions, the values of *a* obtained with *Se* equal to 1 were larger than that obtained with the lower *Se* value meaning that the interfacial area increased with SDS concentrations. With SDS/MCC solutions the interfacial area remains larger than that of water as bubble slip velocities and bubble sizes are lower, giving important gas holdup and interfacial area.

To better understand the effect of the microcrystalline cellulose and its combination with surfactants on the mass transfer phenomena, the volumetric mass transfer coefficient and the liquid-side mass transfer coefficient are considered separately in the next part.

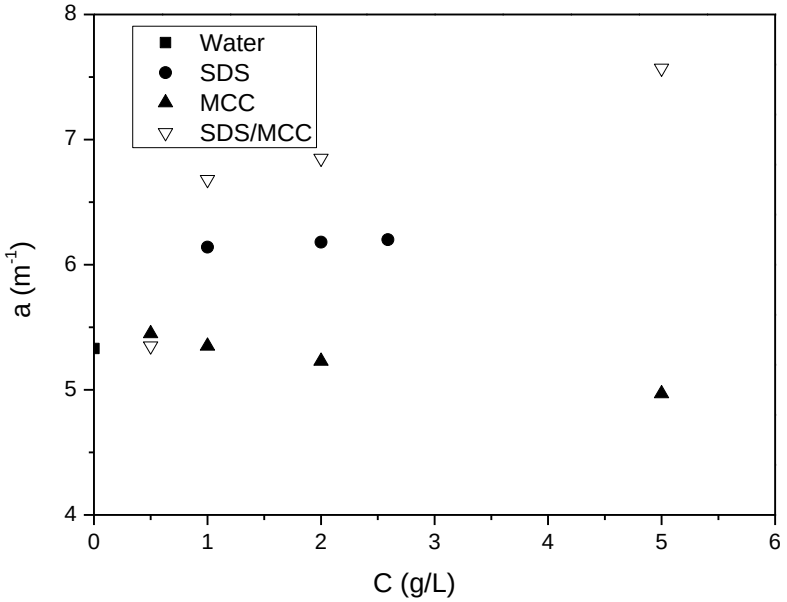

Figure 7. Interfacial area versus the liquid phase concentration

Variation of the volumetric mass transfer coefficient with the liquid phase concentration for the different solutions is plotted in Figure 8. The result indicates that the values of k_La vary between 1.20×10^{-3} and 1.36×10^{-3} s^{-1} for solutions containing SDS, 1.70×10^{-3} and 1.92×10^{-3} s^{-1} for MCC solutions and 1.20×10^{-3} and 1.50×10^{-3} s^{-1} for SDS/MCC solutions. It is clearly shown that the volumetric mass transfer coefficients of all solutions were significantly smaller than those of tap water. For MCC and SDS/MCC solutions, the

volumetric mass transfer coefficient decreased as the concentration increases due to the viscosity change and to the presence of antifoam which promoted bubble coalescence and, therefore, reduced the k_La. The similar results concerning the effect of viscosity on k_La were obtained by Ruen-ngam et *al* [27], and Duran et *al* [5]. In addition, for SDS solutions, the lowest k_La values are obtained with the surface coverage ratio at equilibrium equal to 1, which proved that the presence of surfactants, even in small quantities, has important effects on the oxygen mass transfer. In order to comprehensively understand these phenomenon, the liquid-side mass transfer coefficient (k_L) was then performed.

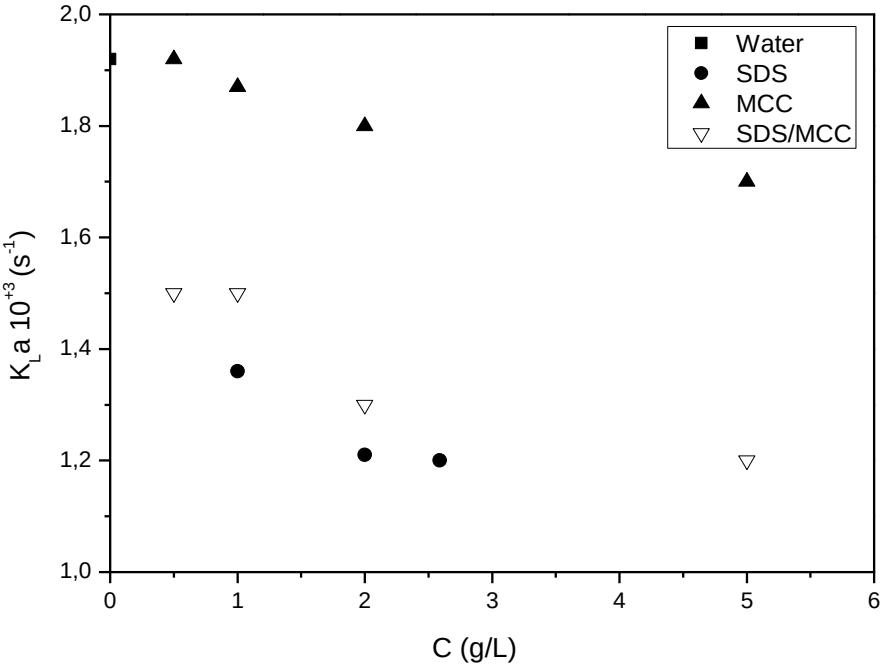

Figure 8. Volumetric mass transfer coefficient versus liquid phase concentration

Relation between the liquid-side mass transfer coefficient and liquid phase concentration for each SDS, MCC and SDS/MCC solutions is shown in Figure 9. The result indicates that the values of k_L varied between 1.97×10^{-4} and 2.21 10^{-4} m.s^{-1} for solutions containing SDS, 3.42×10^{-4} and 3.52×10^{-3} m.s^{-1} for MCC solutions and 1.60×10^{-4} and 2.80×10^{-4} m.s^{-1} for SDS/MCC solutions. It was observed that liquid-side mass transfer coefficients of solutions containing surfactant were significantly smaller than that of water which concord with various literatures [10][14][12]. This decrease can be explained by the fact that the surfactant was assembled at the gas-liquid interface of bubbles. This distribution of surfactants molecules interrupts the mass transfer by modifying the composition and

increasing the thickness of the liquid film around the bubbles. For MCC solutions, it seems that the concentration of the liquid phase do not affect the liquid-side mass transfer coefficient.

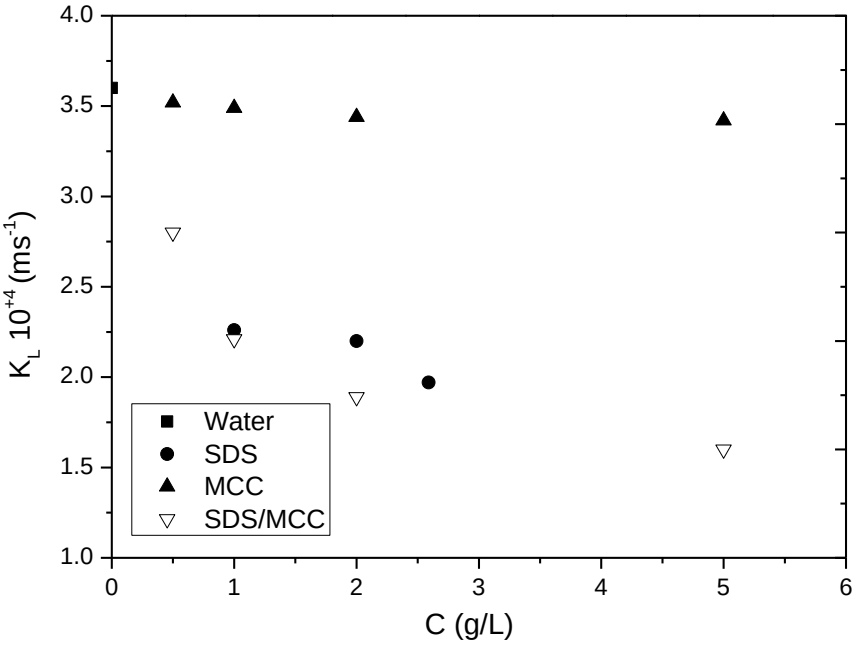

Figure 9. Liquid-side mass transfer coefficient versus liquid phase concentration

Below, superficial gas velocities of 3.66 10^{-4} m/s, 7.73 10^{-4} m/s, 13.33 10^{-4} m/s and 16.66 10^{-4} m/s corresponding respectively to the flow rates of 0.55 ml/s, 1.16 ml/s, 2 ml/s and 2.5 ml/s were studied to understand the influence of superficial gas velocity on hydrodynamic and mass transfer parameters with the presence of surfactants. Tap water, SDS2.59, MCC0.5 and SDS/MCC0.5 are liquid-phases chosen to be studied in this part.

The variation of the bubble diameters in the bubble column as a function of the superficial gas velocity is shown in Figure 10. The values of D_B obtained in this work are in the range of 2 to 5 mm. As it can be observed, whatever the liquid phases, the mean bubble size increases with increasing superficial gas velocity. This result is in accordance with that reported by Loubiere et al [10] for flexible membrane sparger where an increase in gas flow rate lead to enlarge the flexible hole punctured into the membrane. That can also be explained by increase in dispersion of small bubbles within the system with increasing aeration rate and increasing the bubble collision frequency, that leads to higher coalescence rate and an increase in bubble diameter [28]. Figure 12 also illustrates that the addition SDS and MCC to

water reduces the bubble size. This decrease can be attributed to the changes in surface tension and viscosity for SDS and MCC solutions respectively as mentioned earlier in the previous section.

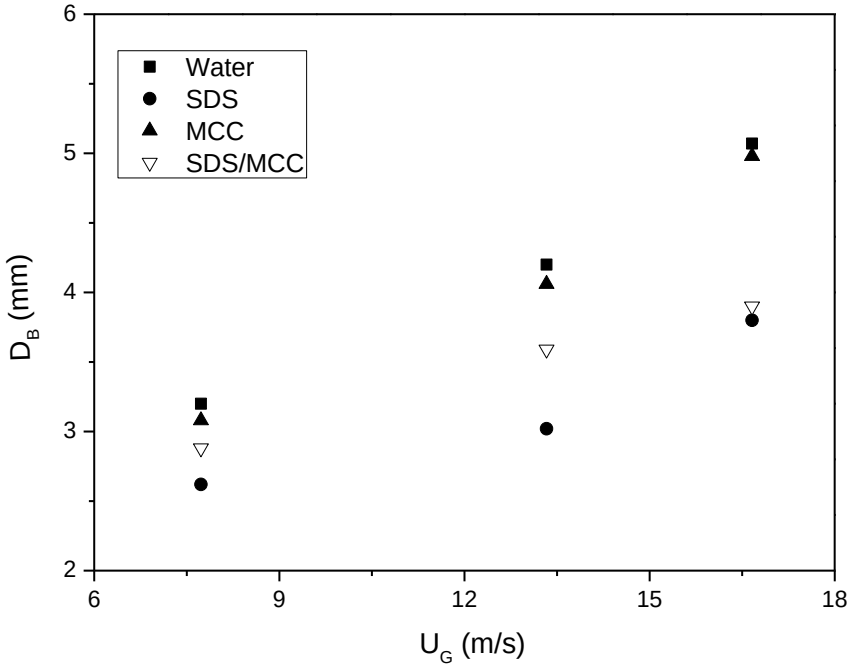

Figure 10. Bubble diameter versus superficial gas velocity

Figure 11 presents the variation of the terminal rising bubble velocity as a function of superficial gas velocity. Result shows that whatever the liquid composition, the terminal rising bubble velocity increase with the superficial gas velocity. As found by Duran et *al* [5], the multiple regression analysis did not show a statistically significant impact of the anionic surfactant SDS and the suspended matter MCC studied on the oxygen transfer coefficient. Nevertheless, the dissolved substances can participate to the depletion of the oxygen transfer coefficient by reducing the bubbles terminal rise velocity [12] [9].

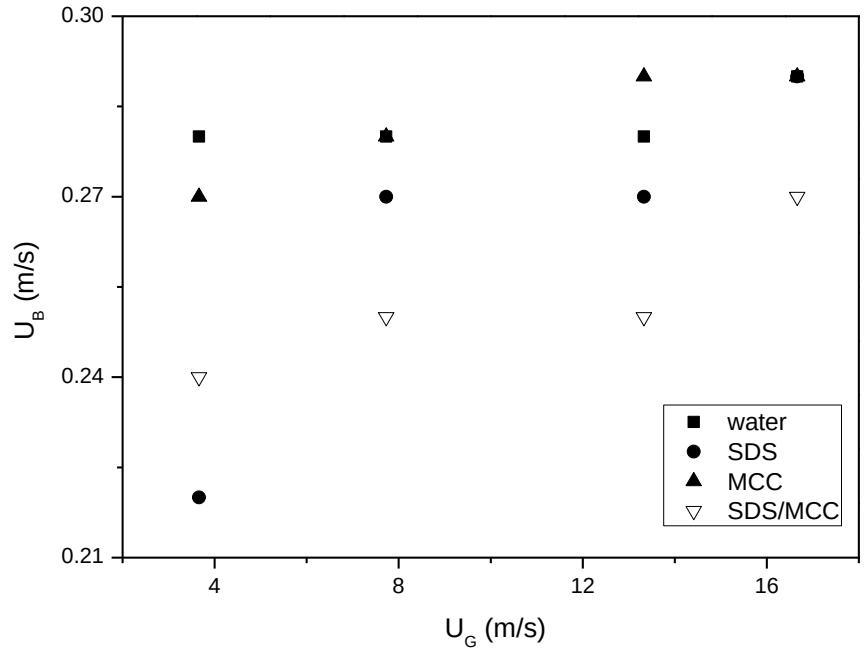

493

494 Figure 11. Terminal rising bubble velocity versus superficial gas velocity

495

496 Variation of the experimental gas–liquid interfacial area with superficial gas velocity is
497 illustrated in Figure 12. As it can be observed, the interfacial area increases with increasing
498 the superficial gas velocity certainly by increasing in gas hold-up. Except for MCC and SDS
499 solutions at low superficial gas velocity, Figure 13 reveals that the interfacial area of the SDS,
500 MCC and their combination in aqueous solutions is larger than that of tap water. Increasing
501 the MCC and SDS concentration reduces the bubble size due to decrease in surface tension.
502 The surface tension has been related to the interfacial area through its effect on bubble size
503 [28].

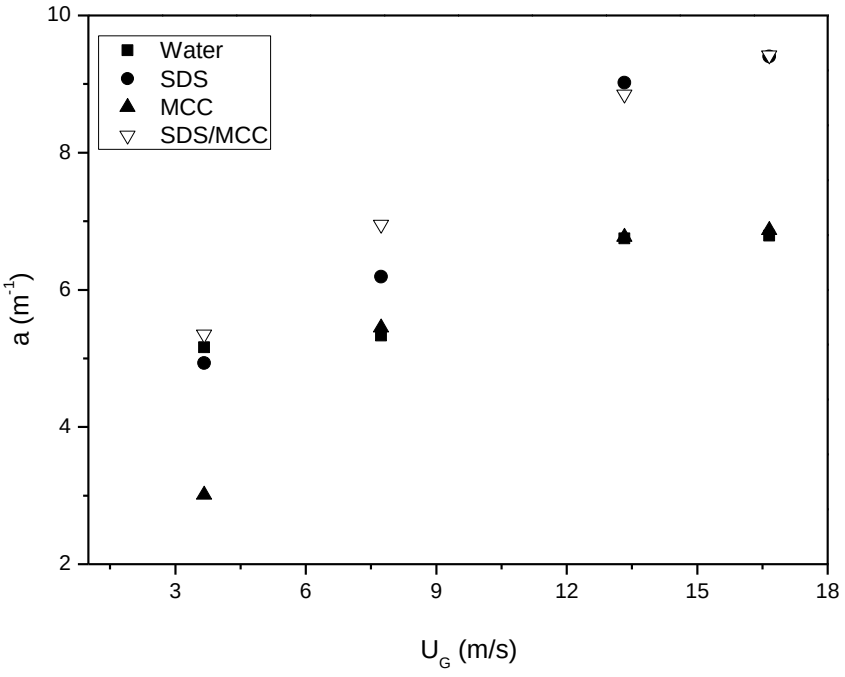

Figure 12. Interfacial area versus superficial gas velocity

Figure 13 presents the variation of volumetric oxygen transfer coefficient for the liquid phases under study as a function of superficial gas velocity. As it can be observed in this figure, except for MCC solutions at high superficial gas velocity, the volumetric oxygen transfer coefficients of the SDS, MCC and their combination in aqueous solutions are lower than that of tap water. It is also observed that the value of k_La for all of liquids increases with the superficial gas velocity which can be mainly explained by an increment in the gas hold up and therefore a larger specific interfacial area. This result corresponds to the homogeneous regime, where k_La increases with the gas velocity [29]. Knowing that the flow rate varies proportionally with the superficial gas velocity, the same results on the k_La were observed by De Jesus et *al* by increasing the flow rate [5]. Besides, the results showed that the volumetric oxygen transfer coefficient is mostly impacted by the MCC and SDS concentration and by superficial gas velocity.

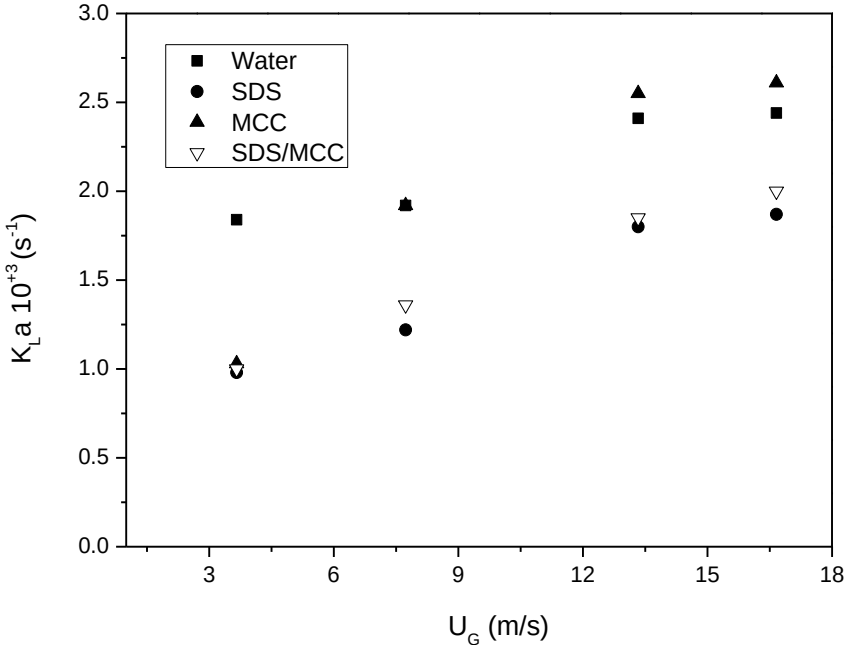

519

520 Figure 13. Volumetric mass transfer coefficient versus superficial gas velocity

521

522 Figure 14 demonstrates the effect of superficial gas velocity on liquid-side mass transfer
523 coefficient. It seems that for a given liquid phase, the superficial gas velocity do not affect the
524 liquid-side mass transfer coefficient. As shown in this figure, by addition of surfactant to
525 water, the mass transfer coefficient decreases. The presence of surfactants over a gas–liquid
526 interface increases the interfacial area by reducing the average bubble diameter, but decreases
527 the mass transfer coefficient by increasing the liquid phase mass transfer resistance. Indeed,
528 the presence of surface contaminants can bring to a lower degree of turbulence in the liquid
529 film around bubbles and a reduction of liquid renewal at interface, therefore, increasing the
530 liquid phase mass transfer resistance [13]. It can also bring to a reduction of diffusion
531 coefficient at the film made at the gas liquid interface where the surfactants can be
532 accumulated [15]. According to Figure 15, the addition of MCC to water and to SDS solution,
533 doesn't modify the mass transfer coefficient. To better understand the effect of MCC on the
534 liquid-side mass transfer coefficient, it should be important to study their presence in other
535 liquid phases and follow by colorimetric technics their behavior at the interface.

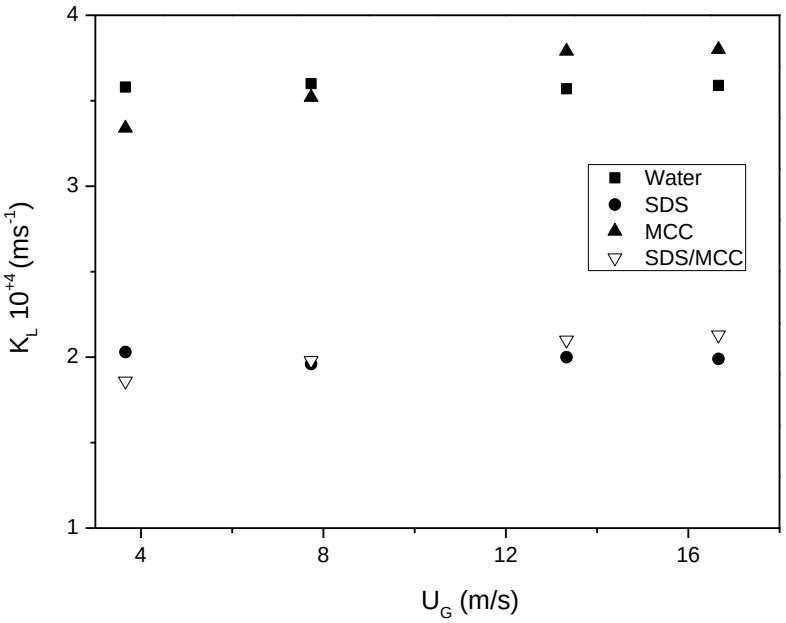

536

537 Figure 14. Liquid-side mass transfer coefficient versus superficial gas velocity

538

539 ## *4.* CONCLUSION

540 The objective of this study was to investigate the effect of surfactants, microcrystalline
541 cellulose and their combination on the hydrodynamic behavior and the mass transfer
542 parameters of a bubble column. Rheological measures showed that an increase in MCC
543 concentration causes an increment in apparent viscosity and accentuates the shear thinning
544 behavior. However, it doesn't affect the liquid-side mass transfer coefficient. It was shown
545 that the presence of surfactants affects the bubble generation process, hence the interfacial
546 area and the different mass transfer parameters. Indeed, the addition of surfactant to water or
547 to MCC in water system decreases the mass transfer coefficient. The k_{La} value for MCC
548 solutions and the k_{La} and k_L value of surfactant solutions were shown to be significantly
549 smaller than those of water. The volumetric mass transfer coefficient was shown to be
550 increased with the superficial gas velocities whatever the liquid phases. However, it seems
551 that for a given liquid phase, the superficial gas velocity doesn't affect the liquid-side mass
552 transfer coefficient. In future work, it should be important to study the presence of surfactant
553 and cellulose in other liquid phases to better understand their effect on the hydrodynamic
554 behavior and liquid-side mass transfer coefficient.

555

ACKNOWLEDGMENTS

The first author gratefully acknowledges “Ministère de l’Enseignement Supérieur et de la Recherche Scientifique, Algérie” and “Institut National des Sciences Appliquées, Toulouse” for the financial support of this work.

REFERENCES

[1] S. M. Walke and V. S. Sathe, “Experimental Study on Comparison of Rising Velocity of Bubbles and Light Weight Particles in the Bubble Column,” *Int. J. Chem. Eng. Appl.*, vol. 3, no. 1, pp. 25–30, 2012.

[2] A. T. A.C.Ahmia, M.Idouhar, O.Arous, K.Sini, A.Ferradj, “Monitoring of Anionic Surfactants in a Wastewater Treatment Plant of Algiers Western Region by a Simplified Spectrophotometric Method,” *J. Surfactants Deterg. 1*, 2016.

[3] M. Bouaifi, G. Hebrard, D. Bastoul, and M. Roustan, “A comparative study of gas hold-up, bubble size, interfacial area and mass transfer coefficients in stirred gas–liquid reactors and bubble columns,” *Chem. Eng. Process. Process Intensif.*, vol. 40, no. 2, pp. 97–111, 2001.

[4] M. Jimenez, N. Dietrich, J. R. Grace, and G. Hébrard, “Oxygen mass transfer and hydrodynamic behaviour in wastewater: Determination of local impact of surfactants by visualization techniques,” *Water Res.*, vol. 58, pp. 111–121, 2014.

[5] C. Durán, Y. Fayolle, Y. Pechaud, A. Cockx, and S. Gillot, “Impact of suspended solids on the activated sludge non-newtonian behaviour and on oxygen transfer in a bubble column,” *Chem. Eng. Sci.*, vol. 141, pp. 154–165, 2016.

[6] X. Zhou, Y. Wu, H. Shi, and Y. Song, “Evaluation of oxygen transfer parameters of fine-bubble aeration system in plug flow aeration tank of wastewater treatment plant,” *J. Environ. Sci.*, vol. 25, no. 2, pp. 295–301, 2013.

[7] K. Sini, M. Idouhar, A.-C. Ahmia, A. Ferradj, and A. Tazerouti, “Spectrophotometric determination of anionic surfactants: optimization by response surface methodology and application to Algiers bay wastewater,” *Environ. Monit. Assess.*, vol. 189, no. 12, p. 646, Nov. 2017.

[8] K. Loubière and G. Hébrard, “Influence of liquid surface tension (surfactants) on bubble formation at rigid and flexible orifices,” *Chem. Eng. Process. Process Intensif.*, vol. 43, no. 11, pp. 1361–1369, 2004.

[9] J. M. T. Alves, S. S. Ovalho, S. P., Vasconcelos, “Effect of bubble contamination on rise velocity and mass transfer,” *Chem. Eng. Sci.*, vol. 60, no. 1, pp. 1–9, Jan. 2005.

[10] P. Painmanakul, K. Loubière, G. Hébrard, M. Mietton-Peuchot, and M. Roustan, “Effect of surfactants on liquid-side mass transfer coefficients,” *Chem. Eng. Sci.*, vol. 60, no. 22, pp. 6480–6491, 2005.

[11] D. Rosso, D. L. Huo, and M. K. Stenstrom, “Effects of interfacial surfactant contamination on bubble gas transfer,” *Chem. Eng. Sci.*, vol. 61, no. 16, pp. 5500–5514, 2006.

[12] R. Sardeing, P. Painmanakul, and G. Hébrard, “Effect of surfactants on liquid-side mass transfer coefficients in gas–liquid systems: A first step to modeling,” *Chem. Eng. Sci.*, vol. 61, no. 19, pp. 6249–6260, 2006.

[13] G. Hebrard, J. Zeng, and K. Loubiere, “Effect of surfactants on liquid side mass transfer coefficients: A new insight,” *Chem. Eng. J.*, vol. 148, no. 1, pp. 132–138, 2009.

[14] M. Jamnongwong, K. Loubiere, N. Dietrich, and G. Hébrard, “Experimental study of oxygen diffusion coefficients in clean water containing salt, glucose or surfactant: Consequences on the liquid-side mass transfer coefficients,” *Chem. Eng. J.*, vol. 165, no. 3, pp. 758–768, 2010.

[15] S. Takagi and Y. Matsumoto, “Surfactant Effects on Bubble Motion and Bubbly Flows,” *Annu. Rev. Fluid Mech.*, vol. 43, no. 1, pp. 615–636, 2011.

[16] K. Mariam, K. Issam, and B. E. N. M. Lassaad, “Bubble hydrodynamic influence on oxygen transfer rate at presence of cationic and anionic surfactants in electroflotation process *,” *J. Hydrodyn.*, vol. 25, no. 5, pp. 747–754, 2013.

[17] D. D. McClure, A. C. Lee, J. M. Kavanagh, D. F. Fletcher, and G. W. Barton, “Impact of Surfactant Addition on Oxygen Mass Transfer in a Bubble Column,” *Chem. Eng.*

Technol., vol. 38, no. 1, pp. 44–52, Jan. 2015.

[18] A. Aoki, J. , Hayashi, K. , Tomiyama, “Mass transfer from single carbon dioxide bubbles in contaminated water in a vertical pipe,” *Int. J. Heat Mass Transf*, vol. 83, no. 0, pp. 652–658, 2015.

[19] M. Haghnegahdar, S. Boden, and U. Hampel, “Investigation of surfactant effect on the bubble shape and mass transfer in a milli-channel using high-resolution microfocus X-ray imaging,” *Int. J. Multiph. Flow*, vol. 87, pp. 184–196, 2016.

[20] C. J. Ruiken, G. Breuer, E. Klaversma, T. Santiago, and M. C. M. van Loosdrecht, “Sieving wastewater - Cellulose recovery, economic and energy evaluation,” *Water Res.*, vol. 47, no. 1, pp. 43–48, 2013.

[21] L. K. Voon, S. C. Pang, and S. F. Chin, “Regeneration of cello-oligomers via selective depolymerization of cellulose fibers derived from printed paper wastes,” *Carbohydr. Polym.*, vol. 142, pp. 31–37, 2016.

[22] P. Milan and R. Campbell W, “The specific interfacial area in externalcirculation- loop airlifts and a bubble column-ii. Carboxymethyl cellulose/sulphite solution,” *Chem. Sci.*, vol. 42, no. 12, p. 2 825-2832, 1987.

[23] C. J.-Y. L. Guo-Qing, Y. Shou-Zhi, C. Zhao-Ling, “Mass transfer and gas–liquid circulation in an airlift bioreactor with viscous non-newtonian fluid,” *Chem. Eng. J. Biochem. Eng. J.*, vol. 56, pp. B101–B107, 1995.

[24] J. M. T. Vasconcelos, J. M. L. Rodrigues, S. C. P. Orvalho, S. S. Alves, R. L. Mendes, and A. Reis, “Effect of contaminants on mass transfer coefficients in bubble column and airlift contactors,” *Chem. Eng. Sci.*, vol. 58, no. 8, pp. 1431–1440, 2003.

[25] K. M. Roberts, D. M. Lavenson, E. J. Tozzi, M. J. McCarthy, and T. Jeoh, “The effects of water interactions in cellulose suspensions on mass transfer and saccharification efficiency at high solids loadings,” *Cellulose*, vol. 18, no. 3, pp. 759–773, 2011.

[26] “Grace, J.R., Wairegi, T., 1986. Properties and Characteristics of Drops and Bubbles. Encyclopedia of Fluid Mechanics, Cheremisinoff. Gulf Publishing Corporation, Huston, TX, pp. 43 – 57 (Chapter 3).,” vol. 57, no. Chapter 3, p. 1986, 1986.

[27] D. Ruen-ngam, P. Wongsuchoto, A. Limpanuphap, T. Charinpanitkul, and P. Pavasant, "Influence of salinity on bubble size distribution and gas-liquid mass transfer in airlift contactors," *Chem. Eng. J.*, vol. 141, no. 1–3, pp. 222–232, 2008.

[28] R. Schäfer, C. Merten, and G. Eigenberger, "Bubble size distributions in a bubble column reactor under industrial conditions," *Exp. Therm. Fluid Sci.*, vol. 26, no. 6–7, pp. 595–604, 2002.

[29] M. Asgharpour, M. R. Mehrnia, and N. Mostoufi, "Effect of surface contaminants on oxygen transfer in bubble column reactors," *Biochem. Eng. J.*, vol. 49, no. 3, pp. 351–360, 2010.